THE FRACTIONAL STEP METHOD APPLIED TO SIMULATIONS OF NATURAL CONVECTIVE FLOWS

Douglas G. Westra
NASA Marshall Space Flight Center

Dr. Juan C. Heinrich
Professor, Aerospace and Mechanical Engineering Department, University of Arizona

ABSTRACT

This paper describes research done to apply the Fractional Step Method to finite-element simulations of natural convective flows in pure liquids, permeable media, and in a directionally solidified metal alloy casting.

The Fractional Step Method has been applied commonly to high Reynold's number flow simulations, but is less common for low Reynold's number flows, such as natural convection in liquids and in permeable media. The Fractional Step Method offers increased speed and reduced memory requirements by allowing non-coupled solution of the pressure and the velocity components.

The Fractional Step Method has particular benefits for predicting flows in a directionally solidified alloy, since other methods presently employed are not very efficient. Previously, the most suitable method for predicting flows in a directionally solidified binary alloy was the penalty method. The penalty method requires direct matrix solvers, due to the penalty term. The Fractional Step Method allows iterative solution of the finite element stiffness matrices, thereby allowing more efficient solution of the matrices. The Fractional Step Method also lends itself to parallel processing, since the velocity component stiffness matrices can be built and solved independently of each other.

The finite-element simulations of a directionally solidified casting are used to predict macrosegregation in directionally solidified castings. In particular, the finite-element simulations predict the existence of "channels" within the processing mushy zone and subsequently "freckles" within the fully processed solid, which are known to result from macrosegregation, or what is often referred to as thermo-solutal convection. These freckles cause material property non-uniformities in directionally solidified castings; therefore many of these castings are scrapped.

The phenomenon of natural convection in an alloy under-going directional solidification, or thermo-solutal convection, will be explained. The development of the momentum and continuity equations for natural convection in a fluid, a permeable medium, and in a binary alloy undergoing directional solidification will be presented. Finally, results for natural convection in

a pure liquid, natural convection in a medium with a constant permeability, and for directional solidification will be presented.

INTRODUCTION

Natural convection occurs in many physical situations. Its most common occurrence arises from an unstable thermal gradient in a gas or liquid. Thermally driven natural convection can also occur in permeable media. Natural convection can also occur in much more complex situations, such as in a liquid metal alloy undergoing directional solidification. Here, the driving force can be thermal, but density differences driven by concentration differences in the liquid can also occur.

The ultimate goal of the work described here was to develop a mathematical model and subsequently the capability to simulate the fluid flows occurring in a directionally solidifying alloy, using the fractional step method. The fundamental equations describing flow in a directionally solidifying alloy are very complicated. In addition, implementation of the fractional step method is challenging. For this reason, the fractional step method was first applied to the equations governing natural convection in a single-phase fluid that can be treated as containing only a single constituent. Next, the fractional step method was applied to the equations governing natural convection in a permeable medium, also containing a single-phase fluid of one constituent. Application of the fractional step method to the simulation of this type of physical situation is slightly more complicated than that for a fluid. Finally, the fractional step method was applied to the equations governing natural convection in a binary alloy undergoing directional solidification.

This paper is laid out as follows. The section following discusses the phenomena occurring in a directional solidifying alloy that contribute to natural convection and the reasons for needing to understand the flow. Fundamentals of the fractional step method are discussed next. The application of the fractional step method to the equations governing flow in a fluid and in permeable media is presented next. Presentation of the fractional step method as applied to the equations governing flow in a binary alloy undergoing directional solidification follows. Next, results of the simulations for the three different flow situations are presented. Finally, conclusions will be discussed.

DIRECTIONAL SOLIDIFICATION

DEFECTS IN ALLOYS AND THEIR CAUSES

Directional solidification is a process by which aircraft engine turbines are produced. Casting defects often necessitate that the entire casting be scrapped, which is very costly. A major defect that leads to scrapped castings is that of concentration non-uniformities. These casting non-uniformities are a direct result of the phenomena occur during the solidification process and affect the consistency and integrity of the casting's structural properties. Two phenomena that

produce concentration non-uniformities and affect their severity are microsegregation and macrosegregation. Microsegregation is a phenomenon that occurs over a distance approaching the size of dendrites in the mushy zone and is dependent on the shape of the dendrites and solute diffusion in the liquid and solid [1]. Macrosegregation causes compositional differences to occur over a distance approaching that of the size of the casting or ingot, and is normally large compared to that caused by diffusion or microsegregation. Consult [1,2,3] for additional information.

During the directional solidification process, the casting is cooled from below. This minimizes convection by imposing a stable temperature gradient. Strictly speaking, due to the stability impressed on the melt by cooling it from below, thermal convection is suppressed. However, depending upon various parameters such as the Solute Rayleigh Number, temperature gradients perpendicular to the gravity vector can interact with the solute field to cause sideways diffusive instability [4,5]. Even more significant is the phenomenon of solute convection occurring when solute rejected at the solidification interface is lighter than the solvent. This combination of phenomena is often referred to as thermosolutal (double diffusive) convection. Thermosolutal convection can cause severe macrosegregation of material.

This severe macrosegregation in the liquid phase causes defects to occur. These defects are made up of long narrow streaks oriented roughly parallel to the direction of gravity. These streaks, or "freckles" have solute concentrations that vary significantly from that of the surroundings [6]. These freckles make the casting more prone to fatigue cracking at the interfaces. Therefore, the castings are scrapped. Several experimental works with nonmetallic transparent systems [7,8] have verified this.

PRESENT SIMULATION CAPABILITIES

Previous research, related to the research proposed herein, as described in Reference [9] has come a long way in simulation of solidification processes. The models currently used by Heinrich et al. [9,10,11,12,13] include interdentritic diffusion, thermosolutal convection, and solute and energy conservation. Since the mushy zone is a metallic dendrite assembly of low, non-uniform, and anisotropic permeability, it is simulated as a region of anisotropic permeability with no predetermined size or shape [14].

Presently, the size of the domains that can be simulated is limited because of the large amount of computer resources required. This limitation is attributed mainly to two issues: 1) In order to adequately capture the diffusion processes occurring in the mushy zone, very fine meshes are required, on the order of dendrite spacing, and 2) since permeability theory is used to model the varying liquid fraction of the mushy zone, the only numerical algorithms that have been successfully employed to solve the momentum equation stiffness matrix are direct solvers.

The penalty method is presently the algorithm employed most frequently for the solution of the solidification momentum equation stiffness matrices. The pressure is not calculated directly in the penalty method formulation. Rather, the pressure term is eliminated by equivalencing it to the continuity equation (which, numerically, has a value very near zero) times a very large

penalty parameter. All velocity components are calculated simultaneously at each time step. Therefore, for a three-dimensional finite-element computation domain consisting of N nodes, the momentum equation stiffness matrix has a size of order 3N X 3N. The stiffness matrix generated by the penalty method requires direct matrix solvers, due to the numerical stiffness introduced by the penalty term and due to the permeability term.
The computer resources required by direct formulations are even more than for the penalty method, since the matrices generated for a direct mixed formulation are non-symmetric. The pressure is calculated with no approximations; therefore there are four unknowns per node, making the stiffness matrix size of order 4N X 4N. Since direct formulations characteristically produce very large ill-formed stiffness matrices, direct formulations are normally used only for calibration of the penalty method and other methods [9].

The Gallerkin Least Squares method was used in the 3D computations described in References [13] and [15], and allowed for large domains to be simulated. However, the use of this method is restricted and very difficult to use.

The attractive feature of the fractional step method is that the velocity components and the pressure can be de-coupled and solved independently. This leads to stiffness matrices that are much smaller and therefore much more manageable. In fact, this allows the solution of flow in large domains that were not realistic previously. The fractional step method is described next.

FUNDAMENTAL PRINCIPLES OF THE FRACTIONAL STEP METHOD

The fractional step method has been used extensively for solution of the incompressible Navier-Stokes equations in Computational Fluid Dynamics (CFD). Chorin [16,17,18] introduced the method over thirty years ago and Temam [19] independently came up with similar ideas. A general description of its implementation is discussed here.

Beginning with the dimensionless form of the incompressible Navier-Stokes equation and continuity:

$$\frac{\mathbf{u}_{n+1}-\mathbf{u}_n}{\Delta t}-\frac{1}{\mathrm{Re}}\nabla^2\mathbf{u}_{n+1}=-\nabla p_{n+1}-\mathbf{u}_n\cdot\nabla\mathbf{u}_n+\mathbf{f}_n \tag{1.1}$$

$$\nabla\cdot\mathbf{u}=0 \tag{1.2}$$

where the velocity has been discretized in time, the viscous and pressure terms are treated implicitly and the convective and forcing term $\mathbf{f}_n$ are treated explicitly. This equation is split into two steps, the intermediate "viscous" step and the projection or "inviscid" step.

$$\frac{\tilde{\mathbf{u}}_{n+1}-\mathbf{u}_n}{\Delta t}-\frac{1}{Re}\nabla^2\tilde{\mathbf{u}}_{n+1}=-\mathbf{u}_n\cdot\nabla\mathbf{u}_n+\mathbf{f}_n \tag{1.3}$$

and

$$\frac{\mathbf{u}_{n+1}-\tilde{\mathbf{u}}_{n+1}}{\Delta t}-\frac{1}{Re}\nabla^2\left(\mathbf{u}_{n+1}-\tilde{\mathbf{u}}_{n+1}\right)=-\nabla p_{n+1} \tag{1.4}$$

The intermediate velocity $\tilde{\mathbf{u}}_{n+1}$ calculated in equation (1.3) does not necessarily meet continuity requirements. This intermediate velocity is corrected in equation (1.4) so that $\mathbf{u}_{n+1}$, the velocity at the end of the time step, does meet continuity. The pressure and subsequently the pressure gradient, are calculated by removing the implicit viscous term in equation (1.4), and then taking the divergence. Due to continuity, equation (1.2), $\nabla\cdot\mathbf{u}_{n+1}$ must vanish and the pressure is obtained from:

$$\nabla^2 p_{n+1}=\frac{\nabla\cdot\tilde{\mathbf{u}}_{n+1}}{\Delta t} \tag{1.5}$$

Removing the implicit viscous term or dealing with it in alternative ways makes the calculation of the pressure much more straightforward. The reason most often cited for removing this term is that the intermediate velocity profile is projected into an "inviscid" vector space, orthogonal to the intermediate "viscous" space [20,21]. Some references treat the viscous term explicitly [22] in equation (1.3) so that it does not appear in equation (1.4). However, explicit treatment of the viscous term restricts numerical stability, particularly for low Reynolds number flow fields. Other references include a more mathematically pure derivation [23,24]. In these references, the fractional step method derived above is modified as follows:

The pressure in equation (1.4) is replaced with $p=\psi-\frac{\Delta t}{Re}\nabla^2\psi$:

$$\frac{\mathbf{u}_{n+1}-\tilde{\mathbf{u}}_{n+1}}{\Delta t}-\frac{1}{Re}\nabla^2\left(\mathbf{u}_{n+1}-\tilde{\mathbf{u}}_{n+1}\right)=-\nabla\left(\psi_{n+1}-\frac{\Delta t}{Re}\nabla^2\psi_{n+1}\right) \tag{1.6}$$

The following terms are removed from equation (1.6) to take on the standard form of the projection step:

$$\frac{\mathbf{u}_{n+1}-\tilde{\mathbf{u}}_{n+1}}{\Delta t}=-\nabla\psi_{n+1} \tag{1.7}$$

Applying the Laplacian Operator to equation (1.7) and multiplying both sides by $\frac{\Delta t}{Re}$ yields an equality for the remaining terms in equation (1.6); therefore removing them is mathematically correct.

Equation (1.5) is now a Poisson equation for ψ instead of p:

$$\nabla^2\psi_{n+1} = \frac{\nabla \cdot \tilde{\mathbf{u}}_{n+1}}{\Delta t} \tag{1.8}$$

and the pressure at the end of the time step is calculated as:

$$p_{n+1} = \psi_{n+1} - \frac{\Delta t}{Re}\nabla^2\psi_{n+1} \tag{1.9}$$

Whether calculating the pressure from equations (1.6), (1.8), and (1.9) is more accurate than calculating it directly from equations (1.3) and (1.5) is application dependent and must be tested in practice [23].

THE ACCURACY OF THE FRACTIONAL STEP METHOD

A number of authors have predicted the accuracy of the fractional step method for incompressible flow [23,24,25,26]. The general consensus is that the velocity can be determined to second-order accuracy. However, there is disagreement on pressure. Some claim the pressure can be determined to second order accuracy [27,28], while others claim that the very nature of the fractional step method limits the pressure to first-order accuracy no matter what steps are taken to improve the method [25,26]. Fortunately, there is consistent agreement on how to improve its accuracy.

The three main methods of ensuring acceptable accuracy for the fractional step method are:

1) Accurate selection of boundary conditions for the intermediate velocity as suggested by Kim and Moin [29].
2) Accurate boundary conditions for the pressure by Orszag et al. [30] and E. and Liu [21,31].
3) Pressure-correction schemes as demonstrated by Van Kan [28], Bell et al. [27], Quartapelle [22], and Gresho [32,33].

The first two items hint at one of the inherent stumbling blocks of the fractional step method [25]. There is only one set of the "real" boundary conditions: the boundary condition for the divergence-free velocity. Since the splitting of the Navier-Stokes equations into two steps requires two sets of boundary conditions, one must be very careful in setting up these boundary conditions.

The third item substitutes the calculation of the pressure at every time step with an "incremental" pressure calculation. That is, the pressure is adjusted or corrected at every time step relative to the previous time step's pressure.

MATHEMATICAL MODEL FOR NATURAL CONVECTION: WITH AND WITHOUT PERMEABILITY

The development of the equations for the solution of Navier-Stokes equations for natural convection in a single-phase, single-constituent fluid and in a permeable medium are very similar. The only difference is the permeability term. Therefore, the development of the equations for a permeable medium are developed here. The equations for natural convection in a fluid can be obtained by removing the permeability term.

DEVELOPMENT OF DIMENSIONLESS MOMENTUM EQUATION FOR NATURAL CONVECTION IN A PERMEABLE MEDIUM

Beginning with the dimensional momentum and continuity equations for a Newtonian Fluid with Constant Density and Constant Viscosity, as found in Appendix C.5 of Panton [34], and with the permeability term added:

$$\rho_0\left(\frac{\partial \mathbf{u}'}{\partial t'}+\mathbf{u}'\cdot\nabla'\mathbf{u}'\right)=-\nabla' p'+\mu\nabla'^2\mathbf{u}'-\mu\left(\mathbf{K}'\right)^{-1}\mathbf{u}'+\rho\,\mathbf{g}' \tag{2.1}$$

$$\nabla'\cdot\mathbf{u}'=0$$

where the permeability vector $\mathbf{K}'$ is defined from the Darcy equation [35]:

$$\mathbf{u}'=-\frac{\mathbf{K}'}{\mu}\left(\nabla' p'-\rho\,\mathbf{g}'\right) \tag{2.2}$$

The primes indicate dimensional terms. Besides the addition of the permeability term, the original Panton equation has been slightly revised (ρ_0 on left hand side) to allow using the Boussinesq approximation [36]. Equation (2.1) shows the permeability term as a vector to account for its anisotropy. For the analysis described in this section, $\mathbf{K}$ is assumed the same in both the x and y directions, therefore, the permeability term will be shown as a scalar term.

For convenience, a component of the hydrostatic pressure (based on the reference density) is separated from the pressure:

$$p'=p'^{*}+\rho_0\left(g_x'x'+g_y'y'\right) \tag{2.3}$$

where p'^{*} is a modified pressure, and the reference density ρ_0 is defined as the density of the fluid at $T = T_0$. The gradient of the pressure can be written as:

$$\nabla' p'=\nabla' p'^{*}+\rho_0\,\mathbf{g}' \tag{2.4}$$

Insert equation (2.4) into equation (2.1) and divide all terms by ρ_0:

$$\frac{\partial \mathbf{u}'}{\partial t'} + \mathbf{u}' \cdot \nabla' \mathbf{u}' = -\frac{1}{\rho_0} \nabla' p'^* - \mathbf{g}' + \nu \nabla'^2 \mathbf{u}' - \nu K^{-1} \mathbf{u}' + \frac{\rho}{\rho_0} \mathbf{g}' \tag{2.5}$$

Now use the Boussinesq approximation for ρ, $\rho = \rho_0 \left[1 + \beta_T \left(T' - T_0'\right)\right]$. The dimensional momentum equation (after canceling the $\mathbf{g}'$ terms) becomes:

$$\frac{\partial \mathbf{u}'}{\partial t'} + \mathbf{u}' \cdot \nabla' \mathbf{u}' = -\frac{1}{\rho_0} \nabla' p'^* + \nu \nabla'^2 \mathbf{u}' - \nu K^{-1} \mathbf{u}' + \beta_T \left(T' - T_0'\right) \mathbf{g}' \tag{2.6}$$

Non-dimensionalize according to the following reference variables:

$$\begin{gathered}
\textit{Characteristic Length } H \\
\textit{Characteristic Velocity } V = \sqrt{\beta_T \, g \, \Delta T \, H} \\
x = \frac{x'}{H}, \quad y = \frac{y'}{H}, \quad \mathbf{u} = \frac{\mathbf{u}'}{V} \\
p^* = \frac{p'^*}{p_0^*} \quad \textit{where} \quad p_0^* = \frac{\rho_0 D_T^2}{H^2} \\
\nabla = \nabla' H \qquad Da = \frac{K}{H^2} \\
\hat{\mathbf{g}} = \frac{\mathbf{g}'}{g} \qquad T = \frac{T' - T_0'}{\Delta T} \\
t = \frac{t'}{\tau} \quad \textit{where} \quad \tau = \frac{H^2}{D_T}
\end{gathered} \tag{2.7}$$

Substituting these terms into Equation (2.6):

$$\frac{V\alpha}{H^2} \frac{\partial \mathbf{u}}{\partial t} + \frac{V^2}{H} \mathbf{u} \cdot \nabla \mathbf{u} = -\frac{D_T^2}{H^3} \nabla p^* + \frac{\nu V}{H^2} \nabla^2 \mathbf{u} - \frac{\nu V}{H^2} Da^{-1} \mathbf{u} + \beta_T \, g \, \Delta T \, T \, \hat{\mathbf{g}} \tag{2.8}$$

Substitute the characteristic velocity V into Equation (2.8):

$$\begin{gathered}
\frac{\sqrt{\beta_T \, g \, \Delta T \, H} D_T}{H^2} \frac{\partial \mathbf{u}}{\partial t} + \beta_T \, g \, \Delta T \, \mathbf{u} \cdot \nabla \mathbf{u} = -\frac{D_T^2}{H^3} \nabla p^* \\
+ \frac{\nu \sqrt{\beta_T \, g \, \Delta T \, H}}{H^2} \nabla^2 \mathbf{u} - \frac{\nu \sqrt{\beta_T \, g \, \Delta T \, H}}{H^2} Da^{-1} \mathbf{u} + \beta_T \, \Delta T \, T \, g \, \hat{\mathbf{g}}
\end{gathered} \tag{2.9}$$

Divide by $\beta_T \, g \Delta T$:

$$\frac{\sqrt{H}D_T}{\sqrt{\beta_T g \Delta T H^2}}\frac{\partial \mathbf{u}}{\partial t}+\mathbf{u}\cdot\nabla\mathbf{u}=-\frac{D_T^2}{\beta_T g \Delta T H^3}\nabla p^* + \frac{\nu\sqrt{H}}{\sqrt{\beta_T g \Delta T H^2}}\nabla^2\mathbf{u}-\frac{\nu\sqrt{H}}{\sqrt{\beta_T g \Delta T H^2}}Da^{-1}\mathbf{u}+T\hat{\mathbf{g}} \tag{2.10}$$

For convenience, drop the * from p and organize according to the following dimensionless parameters:

$$\textit{The Rayleigh Number: } Ra_T=\frac{\beta_T g \Delta T H^3}{\nu D_T}, \qquad \textit{The Prandtl Number: } Pr=\frac{\nu}{D_T} \tag{2.11}$$

This results in the dimensionless momentum equation for natural convection in a permeable medium:

$$\frac{1}{\sqrt{Pr\,Ra_T}}\frac{\partial \mathbf{u}}{\partial t}+\mathbf{u}\cdot\nabla\mathbf{u}=-\frac{1}{Pr\,Ra_T}\nabla p+\sqrt{\frac{Pr}{Ra_T}}\nabla^2\mathbf{u}-\sqrt{\frac{Pr}{Ra_T}}Da^{-1}\mathbf{u}+T\hat{\mathbf{g}} \tag{2.12}$$

The dimensionless continuity equation has the same form as the dimensional version:

$$\nabla\cdot\mathbf{u}=0 \tag{2.13}$$

APPLICATION OF THE FRACTIONAL STEP METHOD TO THE MOMENTUM EQUATION FOR NATURAL CONVECTION IN A PERMEABLE MEDIUM

In order to build stable stiffness matrices for the finite element method, equation (2.12) is rearranged to treat the viscous term and permeability term implicitly and all other terms are moved to the right hand side to be treated explicitly. The fractional step method requires that the transient term be discretized, therefore the subscripts n and n+1 are added, where n refers to the value at the previous time step (known) and n+1 refers to the value at the present time step (unknown).

$$\frac{\mathbf{u}_{n+1}-\mathbf{u}_n}{\Delta t\sqrt{Pr\,Ra_T}}+\sqrt{\frac{Pr}{Ra_T}}Da^{-1}\mathbf{u}_{n+1}-\sqrt{\frac{Pr}{Ra_T}}\nabla^2\mathbf{u}_{n+1}=-\frac{1}{Pr\,Ra_T}\nabla p_{n+1}-\mathbf{u}_n\cdot\nabla\mathbf{u}_n+T_n\hat{\mathbf{g}} \tag{2.14}$$

This is rearranged to the following:

$$\frac{1}{\Delta t\sqrt{\mathrm{Pr}\,\mathrm{Ra_T}}}\left(\mathrm{I}+\Delta\mathrm{t}\,\mathrm{Pr}\,\mathrm{Da}^{-1}-\Delta\mathrm{t}\,\mathrm{Pr}\nabla^2\right)\mathbf{u}_{n+1}=-\frac{1}{\mathrm{Pr}\,\mathrm{Ra_T}}\nabla\mathrm{p}_{n+1}+\mathbf{f}_n \tag{2.15}$$

where the forcing term $\mathbf{f}_n=-\mathbf{u}_n\cdot\nabla\mathbf{u}_n+\mathrm{T}_n\,\hat{\mathbf{g}}+\frac{1}{\Delta t\sqrt{\mathrm{Pr}\,Ra_T}}\mathbf{u}_n$.

Use the equality $p_{n+1}=p_n+(p_{n+1}-p_n)$ to allow calculation of the incremental pressure at every time step. Equation (2.15) then becomes:

$$\frac{1}{\Delta t\sqrt{\mathrm{Pr}\,Ra_T}}\left(I+\Delta t\,\mathrm{Pr}\,Da^{-1}-\theta\,\Delta t\,\mathrm{Pr}\nabla^2\right)\mathbf{u}_{n+1}=-\frac{\left[\nabla p_n+\nabla\left(p_{n+1}-p_n\right)\right]}{\mathrm{Pr}\,Ra_T}+\mathbf{f}_n \tag{2.16}$$

Split Equation (2.16) into a intermediate (viscous) step and a projection (inviscid) step, respectively:

$$\frac{1}{\Delta t\sqrt{\mathrm{Pr}\,Ra_T}}\left(I+\Delta t\,\mathrm{Pr}\,Da^{-1}-\Delta t\,\mathrm{Pr}\nabla^2\right)\tilde{\mathbf{u}}_{n+1}=-\frac{1}{\mathrm{Pr}\,Ra_T}\nabla p_n+\mathbf{f}_n \tag{2.17}$$

$$\frac{1}{\Delta t\sqrt{\mathrm{Pr}\,Ra_T}}\left(I+\Delta t\,\mathrm{Pr}\,Da^{-1}-\Delta t\,\mathrm{Pr}\nabla^2\right)\left(\mathbf{u}_{n+1}-\tilde{\mathbf{u}}_{n+1}\right)=-\frac{1}{\mathrm{Pr}\,Ra_T}\nabla\left(p_{n+1}-p_n\right) \tag{2.18}$$

where $\tilde{\mathbf{u}}_{n+1}$ is the solution to the intermediate step and does not meet continuity. Now, take the divergence of the projection step, equation (2.18):

$$\frac{1}{\Delta t\sqrt{\mathrm{Pr}\,Ra_T}}\nabla\cdot\left\{\left(I+\Delta t\,\mathrm{Pr}\,Da^{-1}-\Delta t\,\mathrm{Pr}\nabla^2\right)\left(\mathbf{u}_{n+1}-\tilde{\mathbf{u}}_{n+1}\right)\right\}=-\frac{1}{\mathrm{Pr}\,Ra_T}\nabla^2\left(p_{n+1}-p_n\right) \tag{2.19}$$

Note that at the end of the time step, the velocity must meet continuity, therefore the divergence of both $\mathbf{u}_{n+1}$ and $\nabla^2\,\mathbf{u}_{n+1}$ are 0:

$$\nabla^2\left(p_{n+1}-p_n\right)=\frac{\sqrt{\mathrm{Pr}\,Ra_T}}{\Delta t}\left(I+\Delta t\,\mathrm{Pr}\,Da^{-1}-\Delta t\,\mathrm{Pr}\nabla^2\right)\nabla\cdot\tilde{\mathbf{u}}_{n+1} \tag{2.20}$$

and the viscous term is ignored:

$$\nabla^2\left(p_{n+1}-p_n\right)=\frac{\sqrt{Pr\,Ra_T}}{\Delta t}\left(I+\Delta t\,Pr\,Da^{-1}\right)\nabla\cdot\tilde{\mathbf{u}}_{n+1} \tag{2.21}$$

To find the divergence-free velocity at the end of the time step, solve for each component of velocity from equation (2.18), again with the viscous term ignored:

$$u_{n+1} = \tilde{u}_{n+1} - \frac{1}{\left(1+\Delta t\, Pr\, Da^{-1}\right)} \frac{\Delta t}{\sqrt{Pr\, Ra_T}} \frac{\partial}{\partial x}\left(p_{n+1} - p_n\right) \tag{2.22}$$

$$v_{n+1} = \tilde{v}_{n+1} - \frac{1}{\left(1+\Delta t\, \mathrm{Pr}\, Da^{-1}\right)} \frac{\Delta t}{\sqrt{\mathrm{Pr}\, Ra_T}} \frac{\partial}{\partial y}\left(p_{n+1} - p_n\right) \tag{2.23}$$

For a pure liquid, the Darcy term K and its dimensionless counter-part Da approach infinity, therefore K^{-1} and Da^{-1} approach zero and can be eliminated from the above equations. In order to solve the above equations numerically, the finite element method is applied. The particular type of finite element method applied is the Gallerkin Method. Consult Heinrich and Pepper [37,38]for details on how the finite element method was applied.

THE FRACTIONAL STEP METHOD APPLIED TO THE MOMENTUM EQUATION FOR DIRECTIONAL SOLIDIFICATION IN A BINARY ALLOY

The above formulation demonstrates the process of applying the fractional step method to a single-constituent, single-phase fluid, with and without permeability. Directional solidification of a binary alloy is much more complicated. This process includes two constituents, two phases and also has anisotropic permeability properties. Developing the formulation here would require considerable space. Therefore, only the results of the formulation are presented. Please consult [9] for more details.

The simulation of directional solidification in a binary alloy includes conservation of energy, species, mass, and momentum balance. Since the fractional step method affects only the conservation of mass and momentum balance, only those equations are presented here. Please consult [9,39,40] for more details regarding the equations for conservation of energy and species.

The dimensionless equation for momentum balance in a directionally solidifying binary alloy is [9]:

$$\begin{aligned} &\frac{\partial \mathbf{u}}{\partial t} + \frac{\phi}{\mathrm{Re}}\mathbf{Da}^{-1}\mathbf{u} - \frac{1}{\mathrm{Re}}\nabla^2\mathbf{u} = -\phi\nabla \mathrm{p} - \frac{1}{\phi}\mathbf{u}\cdot\nabla\mathbf{u} \\ &-\frac{\beta}{\phi}\frac{\partial \phi}{\partial t}\mathbf{u} + \frac{\beta}{3\mathrm{Re}}\nabla\frac{\partial \phi}{\partial t} + \phi\left[\frac{\mathrm{Ra_T}}{\mathrm{Re^2\,Pr}}\mathrm{T} + \frac{\mathrm{Ra_S}}{\mathrm{Re^2\,Sc}}\left(\mathrm{S_L}-1\right)\right]\hat{\mathbf{g}} \end{aligned} \tag{3.1}$$

and the continuity equation is:

$$\nabla\cdot\mathbf{u} = \beta\frac{\partial \phi}{\partial t}. \tag{3.2}$$

where β is the shrinkage coefficient and is defined as $\beta = \frac{\rho_s - \rho_l}{\rho_l}$.

The momentum equation, equation (3.1) is split up into two steps in order to be solved using the fractional step method. The dimensionless equation for the intermediate step is:

$$\frac{1}{\Delta t}\left(1+\frac{\phi\,\Delta t}{\mathrm{Re}}\mathbf{Da}^{-1}\right)\tilde{\mathbf{u}}_{n+1}-\frac{1}{\mathrm{Re}}\nabla^2\tilde{\mathbf{u}}_{n+1}=\mathbf{f}_n-\phi\nabla p_n \tag{3.3}$$

where the (explicit) forcing term $\mathbf{f}_n$ is defined as:

$$\mathbf{f}_n=-\frac{1}{\phi}\mathbf{u}_n\cdot\nabla\mathbf{u}_n-\frac{\beta\,\Delta t}{\phi}\frac{\partial\phi}{\partial t}+\frac{\beta}{3\mathrm{Re}}\nabla\frac{\partial\phi}{\partial t}+\phi\left[\frac{\mathrm{Ra_T}}{\mathrm{Re^2\,Pr}}T+\frac{\mathrm{Ra_S}}{\mathrm{Re^2\,Sc}}(S_L-1)\right]\hat{\mathbf{g}}+\frac{\mathbf{u}_n}{\Delta t} \tag{3.4}$$

The dimensionless equation for the projection step is:

$$\frac{1}{\Delta t}\left(1+\frac{\phi\,\Delta t}{\mathrm{Re}}\mathbf{Da}^{-1}\right)(\mathbf{u}_{n+1}-\tilde{\mathbf{u}}_{n+1})-\frac{1}{\mathrm{Re}}\nabla^2(\mathbf{u}_{n+1}-\tilde{\mathbf{u}}_{n+1})=-\phi\nabla(p_{n+1}-p_n) \tag{3.5}$$

The implicit viscous term is ignored and continuity is imposed by taking the divergence of equation (3.5):

$$\nabla\cdot\left[\sigma\nabla(p_{n+1}-p_n)\right]=\frac{\nabla\cdot\tilde{\mathbf{u}}_{n+1}}{\Delta t}-\frac{\beta}{\Delta t}\frac{\partial\phi}{\partial t} \tag{3.6}$$

where the dimensionless term σ is a function of the fraction liquid ϕ and the anisotropic Darcy term and is a vector quantity:

$$\sigma=\begin{pmatrix}\sigma_x & 0\\ 0 & \sigma_y\end{pmatrix} \tag{3.7}$$

where the individual components of σ are as defined by Sabau, et al. [41]:

$$\sigma_x=\frac{\phi}{1+\dfrac{\phi\,\Delta t}{\mathrm{Re\,Da_x}}},\ \text{and}\ \ \sigma_y=\frac{\phi}{1+\dfrac{\phi\,\Delta t}{\mathrm{Re\,Da_y}}} \tag{3.8}$$

The dimensionless scaling parameters are:

$$\text{The Reynold's Number:} \quad \mathrm{Re} = \frac{VH}{\nu}$$

$$\text{The Thermal Rayleigh Number:} \quad \mathrm{Ra_T} = \frac{\beta_T g G H^4}{\nu D_T}$$

$$\text{The Solute Rayleigh Number:} \quad \mathrm{Ra_S} = \frac{\beta_S g S_0 H^3}{\nu D_S} \tag{3.9}$$

$$\text{The Prandtl Number:} \quad \mathrm{Pr} = \frac{\nu}{D_T}$$

$$\text{The Schmidt Number:} \quad \mathrm{Sc} = \frac{\nu}{D_S}$$

As was done for the case of natural convection in a liquid or a permeable medium, the finite element method was applied in order to solve the above equations numerically.

RESULTS

Steady-state results are presented for natural convection in a fluid and in a permeable medium. Transient results are presented for a binary metal alloy under-going directional solidification.

RESULTS OF SIMULATING THE MOMENTUM EQUATION FOR NATURAL CONVECTION IN A PERMEABLE MEDIUM

Figures 1 – 6 show steady-state simulation results of the fractional step method applied to the momentum equation for natural convection in a fluid and in a permeable medium. Note that Figures 1 – 5 are contour plots of the temperature with the velocity vectors super-imposed. Figure 6 is a contour plot of the pressure for the same case as Figure 5. There are 41 nodes in each direction in all cases presented.
The results are presented in dimensionless form, with a dimensionless area of 1 X 1. The dimensionless temperature is 1.0 at the bottom and 0.0 at the top. The gravity vector is oriented in the minus y direction in all simulations, to create an unstable thermal condition. The gravity vector has a magnitude of 9.81 m/s^2 in all simulations. Table I summarizes these results, listing the dimensionless parameters defined in equation (2.11). Fluid properties are given, along with appropriate scaling parameters that correspond to the Rayleigh Numbers and Prandtl Numbers listed. In two of the cases listed, fluid properties of air and water at 300 K were used. Consult equation (2.7) to determine how reference variables relate to physical dimensions, boundary conditions, and fluid properties.

RESULTS OF SIMULATING THE MOMENTUM EQUATION IN A BINARY ALLOY UNDERGOING DIRECTIONAL SOLIDIFICATION

Figure 7 shows the rectangular simulation domain of a 0.008 m by 0.03 m rectangle for an alloy comprised of 94.2 % Lead, 5.8 % Antimony by weight (Pb-5.8% wt. Sb). A mesh spacing of 0.0002 m is used, which is on the order of the primary dendrite arm spacings. The initial condition consists of a fixed temperature at the bottom boundary (Y' = 0.0) set to the alloy liquidus temperature and an imposed thermal gradient of G_0 = 12,000 K/m (positive with respect to Y') throughout the liquid melt. The liquid melt is of uniform composition S_0 (5.8%). The simulated boundary conditions are an imposed thermal gradient of 12,000 K/m at the top boundary, and 0.36 K/s cooling at the bottom (the temperature at the bottom boundary is changed in time). A uniform body force of 9.81 m/s^2 is imposed in the minus Y' direction. Figure 7(a) shows the three zones that are normally present during solidification: liquid, solid, and mush.

Figures 8 – 11 are simulation results of the fractional step method applied to the momentum equation for natural convection in a binary alloy undergoing directional solidification. In this case, the boundary condition is continually changing and there is not a steady-state condition. The simulated time is 400 seconds in Figure 8 – 12.

Figure 8 shows the temperature and pressure, clearly indicating the imposed temperature gradient and the resulting pressure gradient. Figure 9 shows a plot of the fraction liquid and the concentration of the alloy throughout. The three regions are labeled on the left hand side of Figure 9: "Liquid, "Mush" or mushy zone, and "Solid". At this solidification time, the mushy zone is located approximately between Y = 0.007 and 0.010 meters. The "freckles" on the concentration plot are clearly seen and are a result of thermosolutal convection. The distortion of the fraction liquid from a purely vertical gradient is also obvious and is a direct result of the thermosolutal convection. Figure 10 shows the same plot of fraction liquid and concentration as in Figure 9, with the velocity vectors super-imposed. It is seen that the velocities emanate from the regions of highest deviation from the base concentration of 5.8%. Figure 11 shows a close-up of the velocities and concentration occurring just above the mushy zone. Finally, Figure 12 shows the velocities and concentration occurring in the mushy zone. The code is achieving acceptable continuity when simulating velocities even in the mushy zone, where the magnitude of the velocity is several orders of magnitude smaller than the velocities occurring in the all-liquid region.

CONCLUSIONS

Natural convection is a phenomena common to fluids, permeable media, and also occurs in more complex situations such as in a binary alloy under-going directional solidification. Thermo-solutal convection in castings undergoing directional solidification leads to concentration non-uniformities that necessitate scrapping the castings. The fractional step method has been successfully applied to simulation of natural convection in pure fluids, permeable media, and in a binary alloy undergoing directional solidification. Its use in simulations of directional solidification allows larger domains to be simulated. The results presented here are for two-dimensional domains only. Presently, efforts are underway to extend simulation of directional solidification with the fractional step method to three dimensions.

Table I

Scaling Parameters, Reference Variables, and Fluid Properties for Figures 1- 6

Figure	Ra	Pr	Da	ΔT^a (K)	Fluid Properties	H^a (m)	V^a (m/s)
1	10^5	1.00	N/A	100	See Note b	1.0	0.32
2	10^5	7.00	N/A	100	See Note c	1.0	0.26
3	10^6	0.71	N/A	85	**Air @ 300 K**	0.05	0.38
4	10^6	1.0	10^{-4}	100	See Note d	1.0	0.31
5, 6	10^8	5.83	10^{-6}	20	**Water @ 300 K**	0.06	0.06

a - ReferenceVariables given in equation (2.7).

b - The thermal coefficient of expansion is assumed to be –0.0001 K^{-1}, the kinematic viscosity is assumed to be 10^{-3} m^2/s, and the thermal diffusivity is assumed to be 10^{-3} m^2/s.

c - The thermal coefficient of expansion is assumed to be –0.0001 K^{-1}, the kinematic viscosity is assumed to be 7 X 10^{-4} m^2/s, and the thermal diffusivity is assumed to be 10^{-4} m^2/s.

d - The thermal coefficient of expansion is assumed to be –0.001 K^{-1}, the kinematic viscosity is assumed to be 10^{-3} m^2/s, and the thermal diffusivity is assumed to be 10^{-3} m^2/s .

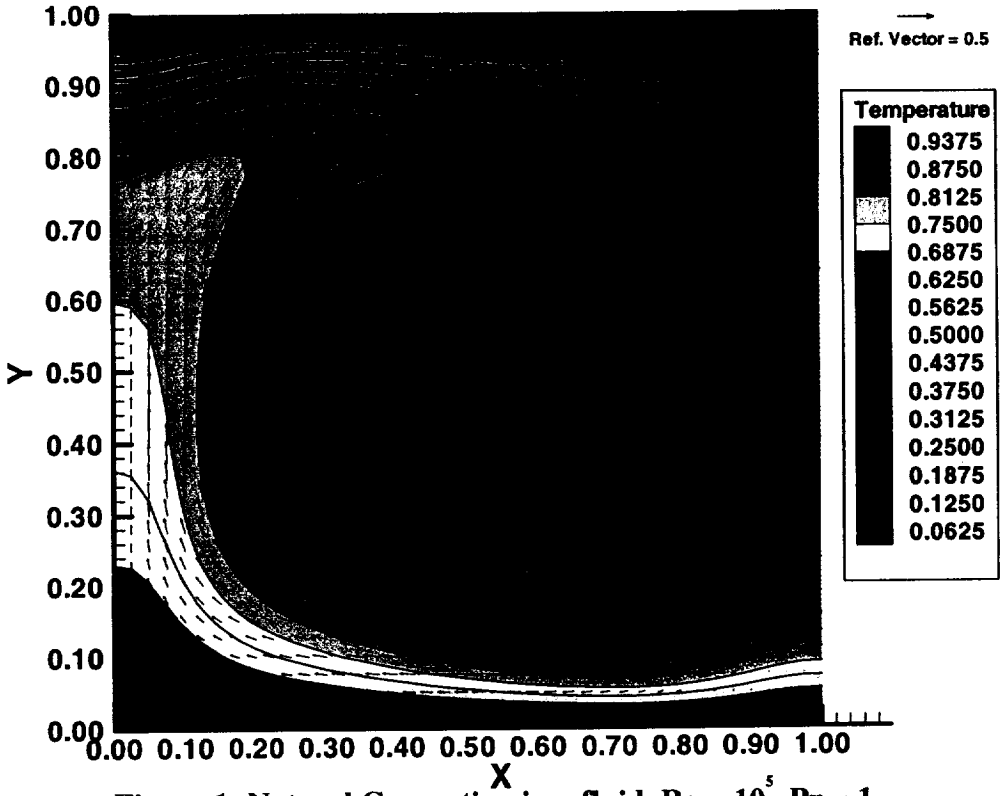

Figure 1: Natural Convection in a fluid, Ra = 10^5, Pr = 1.

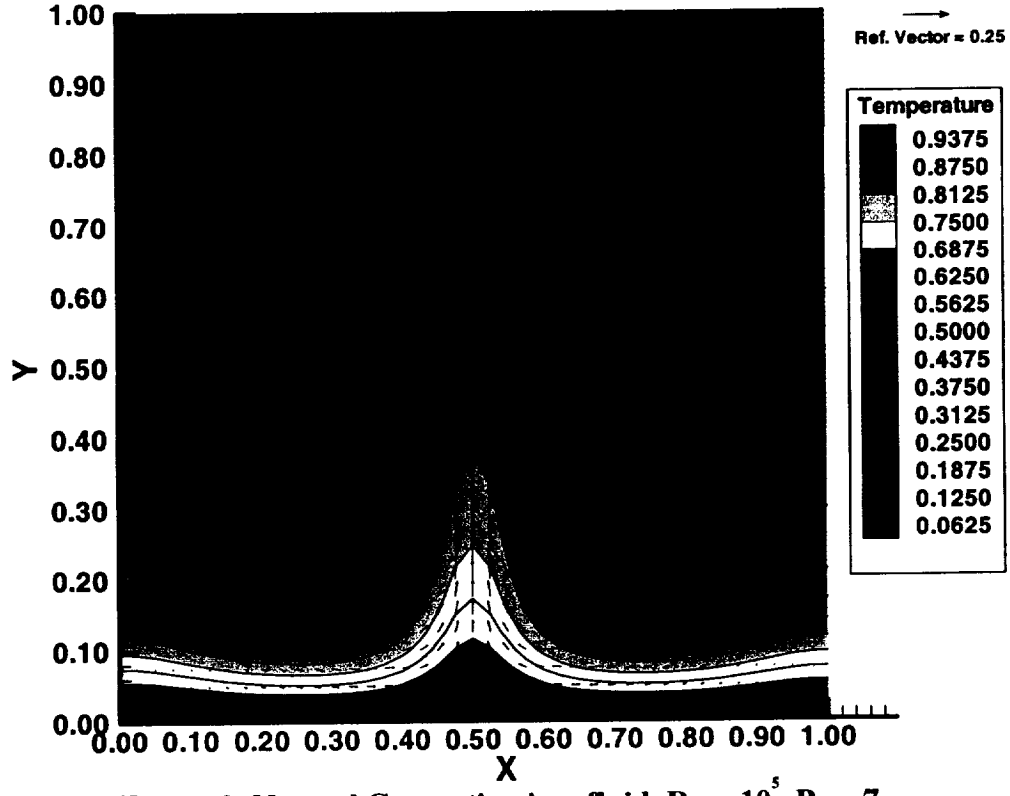

Figure 2: Natural Convection in a fluid, Ra = 10^5, Pr = 7.

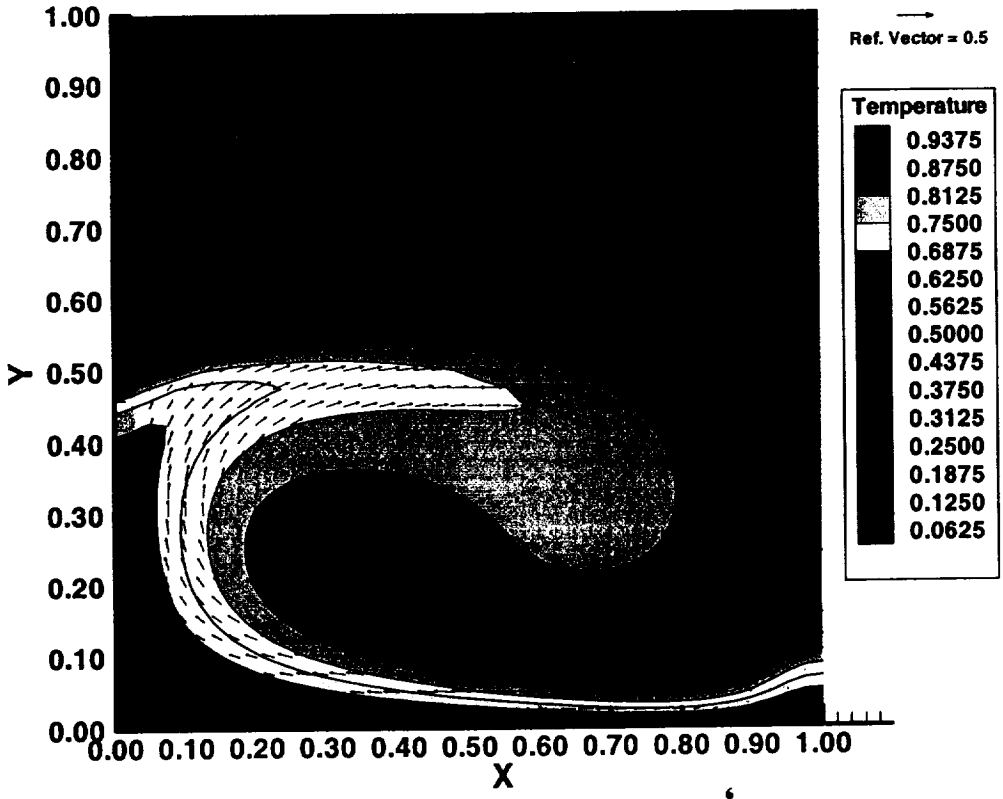

Figure 3: Natural Convection in Air, Ra = 10^6, Pr = 0.71.

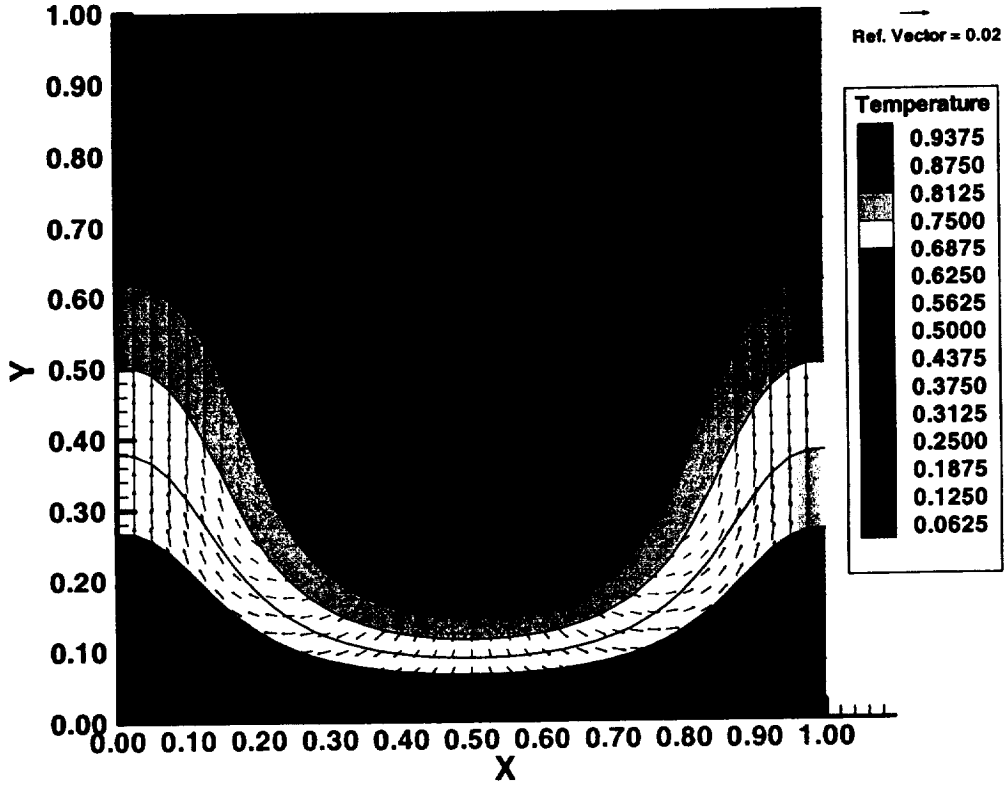

Figure 4: Natural Convection in a Permeable Medium, Ra = 10^6, Pr = 1, Da = 10^{-4}.

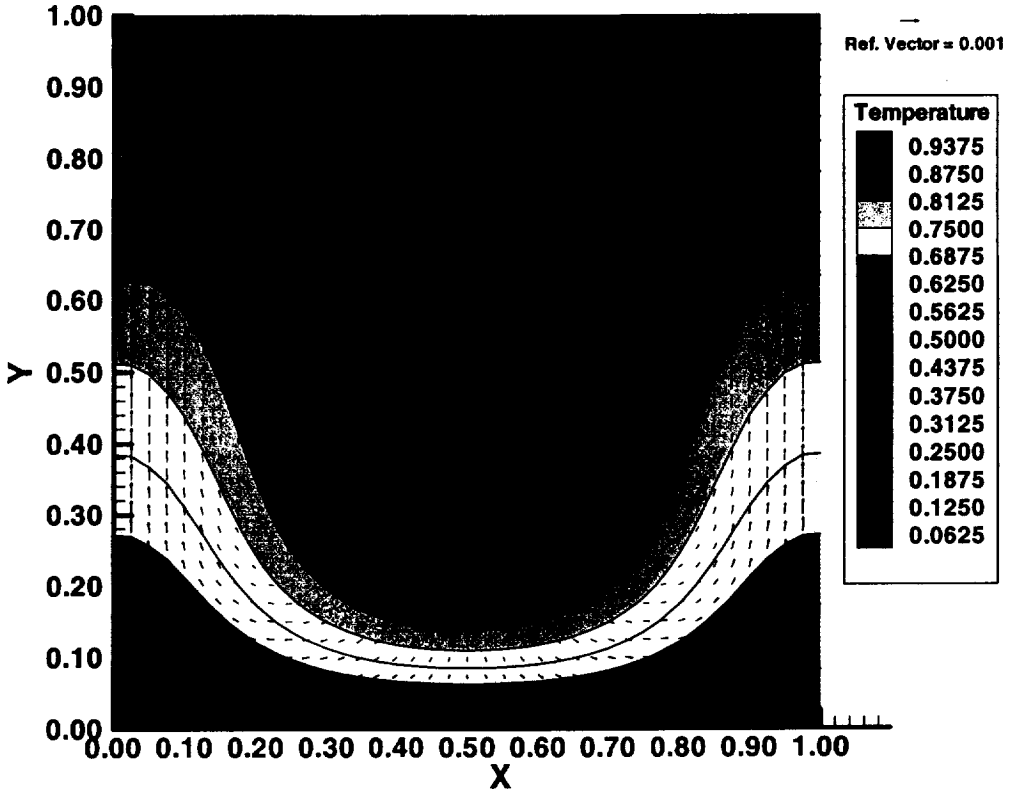

Figure 5: Natural Convection in a Permeable Medium with Water as the Base Fluid. Ra = 10^8, Pr = 1, Da = 10^{-6}.

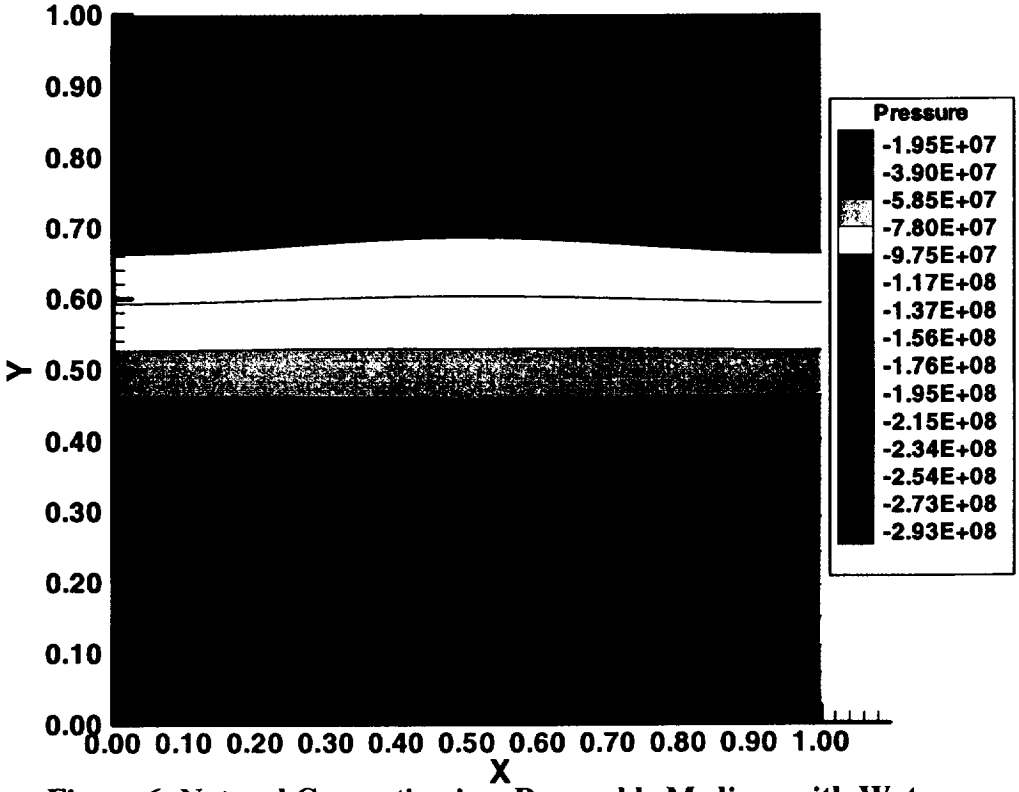

Figure 6: Natural Convection in a Permeable Medium with Water as the Base Fluid. Ra = 10^8, Pr = 1, Da = 10^{-6}.

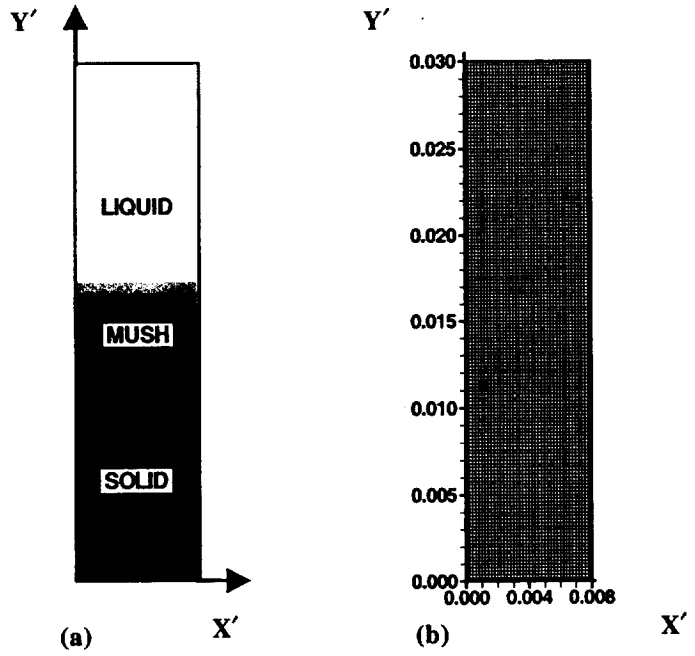

Figure 7. (a) Basic domain and coordinate system for solidification of a binary alloy. (b) Dimensions (m) and mesh spacing of the domain used in the simulations reported here.

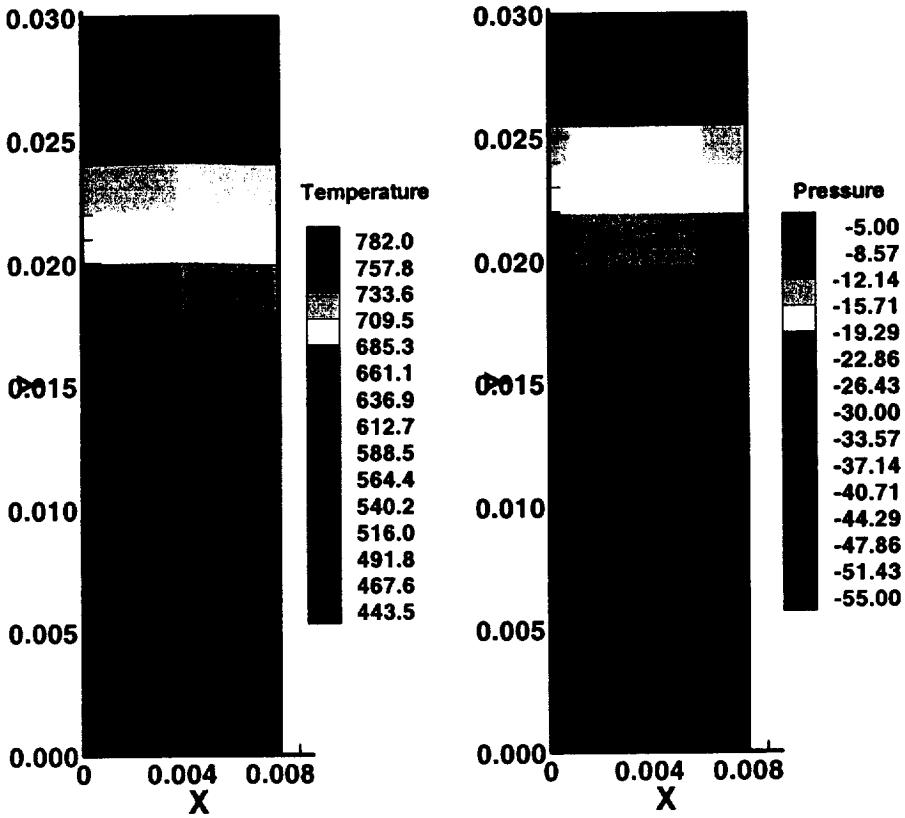

Figure 8. Temperature and Pressure Results for Pb-5.8 wt. % Sb.

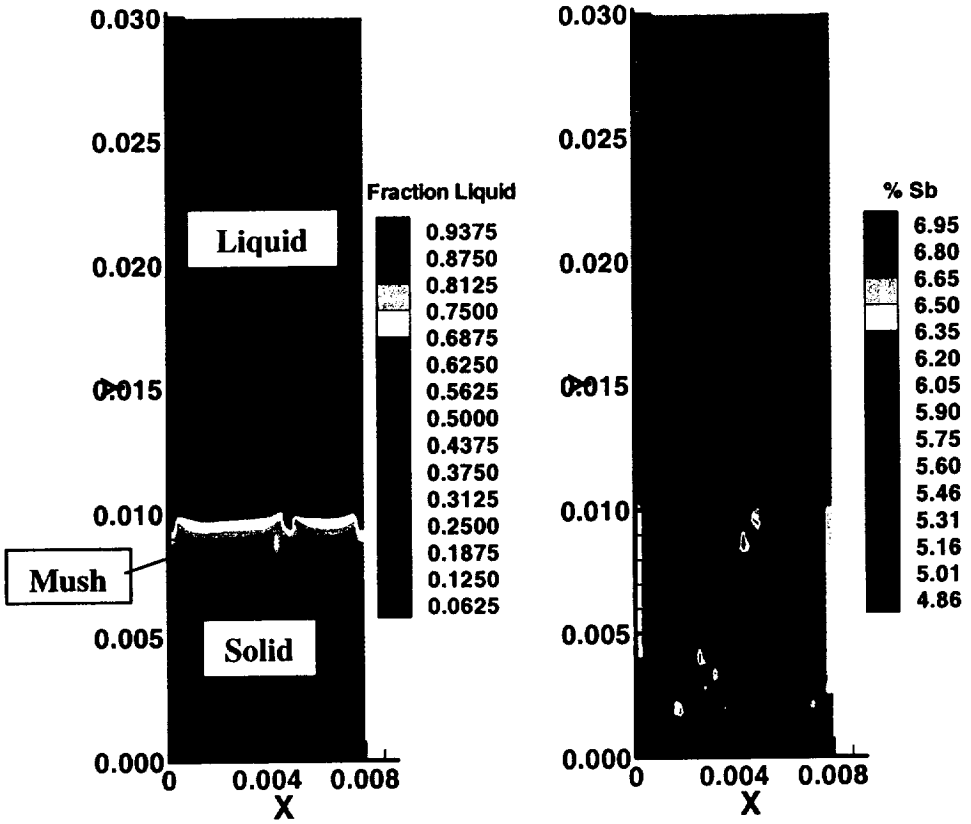

Figure 9. Fraction Liquid and Concentration Results for Pb-5.8 wt. % Sb.

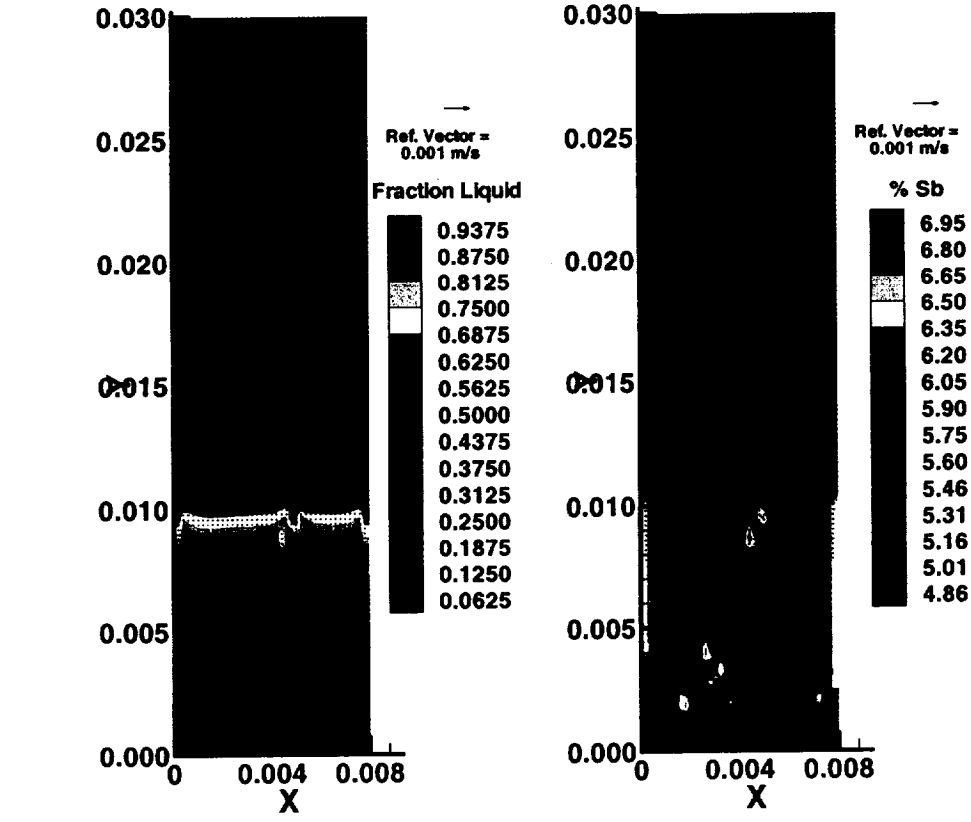

Figure 10. Fraction Liquid and Concentration Results for Pb-5.8 wt. % Sb.

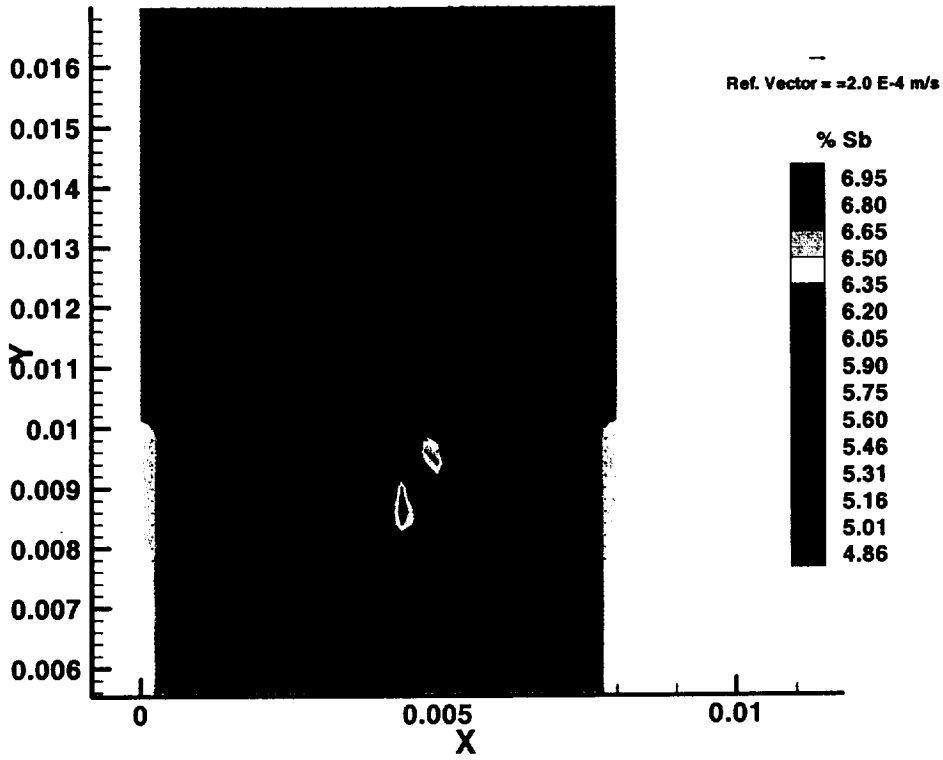

Figure 11. Concentration, Velocity Results near Mushy Zone, for Pb-5.8 wt. % Sb.

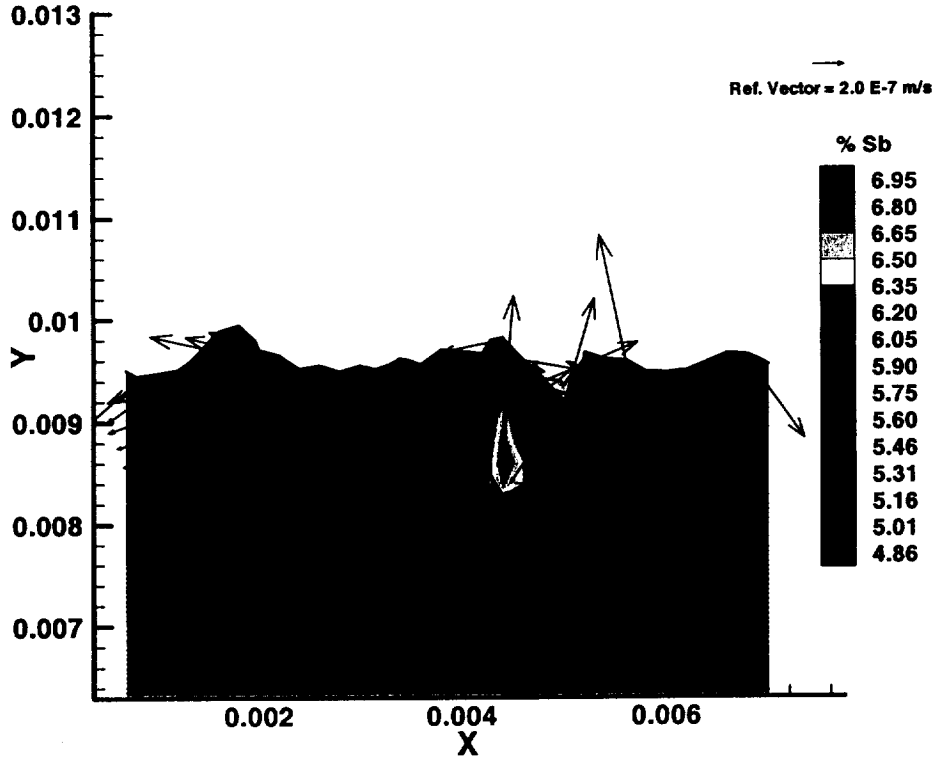

Figure 12. Concentration, Velocity Results inside the Mushy Zone, for Pb-5.8 wt. % Sb.

REFERENCES

[1] Kurz, W. and Fisher, D.J. "Fundamentals of Solidification". Trans Tech Publications. 1992.

[2] Porter, D.A. and Easterling, K.E. "Phase Transformations in Metals and Alloys, Second Edition." Chapman & Hall. 1992.

[3] Flemings, MC. "Solidification processing". McGraw-Hill, New York, NY. 1974.

[4] Favier J.J. "Recent advances in Bridgman growth modeling and fluid flow." *Journal of Crystal Growth* **99**: 18-29 (1990).

[5] Rouzaud A, Camel D, and Favier JJ. "A comparitive study of thermal and thermosolutal convective effects in vertical Bridgman crystal growth." *Journal of Crystal Growth* **73**: 149-166 (1985).

[6] Nandapurkar P., Poirier D.R., Heinrich J.C., and Felicelli S. "Thermosolutal Convection during Dendritic Solidification of Alloys: Part I. Linear Stability Analysis", *Metallurgical Material Transactions B. Numer.* **20B**: 711-721 (1989).

[7] Copley SM, Giamei AF, Johnson SM and Hornbecker MF. *Metallurgical Material Transactions.* **1**: 2193-2204 (1970).

[8] Chen F, and Chen CF. *J .Fluid Mech.* **227**: 567-586 (1991).

[9] Heinrich J.C. and McBride E. "Calculation of pressure in the mushy zone", *Int. J. Numer. Methods Engng.* 47, 735-747 (2000).

[10] McBride E, Heinrich JC, and Poirier DR. "Numerical simulation of incompressible flow driven by density variations during phase change." *Int. J. Numer. Methods in Fluids* **31**: 787-800 (1999).

[11] Felicelli SD, Poirier DR and Heinrich JC. "Finite element analysis of directional solidification of multi-component alloys", *Int. J. Numer. Methods in Fluids* **27**: 207-227 (1998).

[12] Heinrich J.C., Felicelli S., Nandapurkar P., and Poirier D.R., "Thermosolutal Convection during Dendritic Solidification of Alloys: Part II. Nonlinear Convection", *Metallurgical Material Transactions B.* **20B**: 883-891 (1989).

[13] Felicelli S.D., Heinrich J.C., and Poirier D.R., "Three-dimensional simulations of freckles in binary alloys." *Journal of Crystal Growth* **191**: 879-888 (1998).

[14] Felicelli S.D., Heinrich J.C., and Poirier D.R., "Simulation of Freckles during Vertical Solidification of Binary Alloys." *Metallurgical Material Transactions B. Numer.* **22B**: 847-859 (1991).

15] Felicelli SD, Poirier DR and Heinrich JC. "Modeling freckle formation in three dimensions during solidification of multi-component alloys" *Metallurgical Material Transactions B.* **29B**: 847-855 (1998).

[16] Chorin AJ "The numerical solution of the Navier-Stokes equations for an incompressible fluid." *Bull. Amer. Math Soc.* **73**: 928-931 (1967).

[17] Chorin AJ "Numerical solution of the Navier-Stokes equations." *Math Comp.* **22**: 745-762 (1968).

[18] Chorin AJ "On the convergence of discrete approximations to the Navier-Stokes equations." *Math Comp.* **23**: 341-353 (1969).

[19] Temam R. "Sur l'approximation de la solution des equations de Navier-Stokes par la mehode des fractionnarires II. *Arch. Rational Mech Anal.* **33**: 377-385 (1969).

[20] Almgren AS, Bell JB, and Szymczak WG. "A numerical method for the incompressible Navier-Stokes Equations based on an approximate projection." *SIAM J. Sci. Comput.* **17, No. 2**: 358-369 (1996).

[21] E W and Liu J-G. "Projection method I: Convergence and numerical boundary layers." *SIAM Journal of Numerical Analysis.* **32**: 1017-1057 (1995).

[22] Quartapelle L. "Numerical Solution of the Incompressible Navier-Stokes Equations." Birkhauser Verlag, Berlin. 1993.

[23] Shen J. "On error estimates of projection methods for Navier-Stokes equations: First-order schemes. *SIAM J. Numer. Anal.* **29**: 57-77 (1992).

[24] Shen J. "On error estimates of some higher order projection and penalty-projection methods for Navier-Stokes equations: First-order schemes. *Numer. Math.* **62**: 49-73 (1992).

[25] Strikwerda JC and Lee YS. "The accuracy of the fractional-step method". *SIAM Journal of Numerical Analysis.* **37, No. 1**: 37-47 (1999).

[26] Perot JB. "An analysis of the fractional step method." *J. Comput. Phys.* **108**: 51-58 (1993).

[27] Bell JB, Colella P, and Glaz HM. "A second-order projection method for the incompressible Navier-Stokes equations." *J. Comput. Phys.* **85**: 257-283 (1989).

[28] Van Kan J. "A second-order accurate pressure-correction scheme for viscous incompressible flow." *SIAM J. Sci. Stat. Comput.* **7**: 870-891 (1986).

[29] Kim J, and Moin P. Application of a fractional-step method to incompressible Navier-Stokes." *J. Comput. Phys.* **59**: 308-323 (1985).

[30] Orszag SA, Israeli M, and Deville MO. "Boundary conditions for incompressible flows." *Journal of Scientific Computing*. **1**: 75-110. (1986).

[31] E W and Liu J-G. "Projection method II: Godunov-Ryabenki analysis." *SIAM Journal of Numerical Analysis*. **33**: 1597-1621 (1996).

[32] Gresho PM. "On the theory of semi-implicit projection methods for viscous incompressible flow and its implementation via a finite element method that also introduces a nearly consistent mass matrix. Part 1: Theory." *Int. J. for Numer. Methods in Fluids*. **11**: 587-620 (1990).

[33] Gresho PM and Chan ST. "On the theory of semi-implicit projection methods for viscous incompressible flow and its implementation via a finite element method that also introduces a nearly consistent mass matrix. Part 2: Implementation." *Int. J. for Numer. Methods in Fluids*. **11**: 621-659 (1990).

[34] Panton RL. "Incompressible flow." 2nd edition. John Wiley & Sons, Inc. 1995.

[35] Bird RB, Stewart WE, and Lightfoot EN. "Transport Phenomena." John Wiley, New York, NY, 1960, pp. 59 and 150.

[36] Chandrasekhar S. "Hydrodynamic and hydromagnetic stability." Dover Publications, Inc. New York. 1961.

[37] Heinrich JC, and Pepper DW. "Intermediate Finite Element Method, Fluid Flow and Heat Transfer Applications." Taylor & Francis. 1999.

[38] Pepper DW, and Heinrich JC. "The Finite Element Method, Basic Concepts and Applications." Taylor & Francis. 1992.

[39] Ganesan S and Poirier DR. "Conservation of mass and momentum for the flow of interdendritic liquid during solidification." *Metall. Trans.* **21B**: 173-181 (1993).

[40] Poirier DR, Nandapurkar PJ, and Ganesan S. "The energy and solute conservation equations for dendritic solidification." *Metall. Trans.* **22B**: 889-900 (1991).

[41] Sabau AS, Han Q, and Viswanathan S. "Projection Methods for Interdentritic Flows." 128th TMS Annual Meeting & Exhibition. San Diego. 1999.

CONTACT

Douglas G. Westra
NASA / Marshall Space Flight Center
Mail Code ED25
MSFC, AL 35812

(256) 544-3120 (256) 544-0800 (FAX)
doug.westra@msfc.nasa.gov

NOMENCLATURE

Scalars

β	shrinkage coefficient due to phase change from liquid to solid
β_T	coefficient of thermal expansion, 1/K
β_S	coefficient of solute expansion
ρ_0	reference density, kg/m^3
ρ_L	density of liquid, kg/m^3
ρ_S	density of solid, kg/m^3
ϕ	fraction liquid
μ	dynamic viscosity, $N\text{-}s/m^2$
ν	kinematic viscosity, m^2/s
ψ	pressure function, Pa
Da	permeability, dimensionless
D_T	thermal diffusivity, m^2/s
D_S	solute diffusivity, m^2/s
g	value of gravity vector, m/s^2
G	reference thermal gradient, K/m
H	reference length, m
I	Identity Matrix
K	permeability , m^2

p' pressure, Pa

p'^* modified pressure, Pa

Pr Prandtl Number

Re Reynold's Number

Ra_T thermal Rayleigh Number

Ra_S solute Rayleigh Number

Sc Schmidt Number

S_0 reference solute concentration, %

t' time, s

Δt time step size, s

T' temperature, K

ΔT reference temperature difference, K

u' velocity in x direction, m/s

v' velocity in y direction, m/s

V reference velocity, m/s

Vectors

$\mathbf{g}$ gravity vector, m/s^2

$\mathbf{n}$ direction normal to boundary

$\mathbf{t}'$ direction tangent to boundary

$\mathbf{u}'$ velocity vector, m/s